Theory of Z-scan technique using Gaussian–Bessel beams with a phase object*

Jin Xiao(金 肖)[a)b)], Shui Min(税 敏)[a)], Wang Yu-Xiao(王玉晓)[a)],
Li Chang-Wei(李常伟)[a)], Yang Jun-Yi(杨俊义)[b)], Zhang Xue-Ru(张学如)[a)],
Yang Kun(杨 昆)[a)], and Song Ying-Lin(宋瑛林)[a)b)†]

[a)] *Department of Physics, Harbin Institute of Technology, Harbin* 150001, *China*
[b)] *Department of Physics, Soochow University, Soochow* 215006, *China*

(Received 30 November 2009; revised manuscript received 6 January 2010)

This paper reports the theoretical study of combining Z-scan technique with Gauss–Bessel (GB) beams beside a phase object (PO) to measure the third-order nonlinear susceptibility components. By using this method, the sign of refractive index which depends on the shape of the close aperture Z-scan curve can be easily determined. Meanwhile, the magnitude of nonlinear coefficients can also be deduced by theoretical fit. The proposed method is advantageous for high sensitivity and imposes a lower stress in the cases of fragile materials, since small pulse energy is enough for the measurement of nonlinear coefficients. Predictions of the models are compared with Gaussian Z-scan measurement and GB Z-scan measurement. By using GB beams with a PO, the sensitivity of Z-scan measurements is found to be a factor of over 60 times greater than for Gaussian beams and 2 times greater than for Gaussian-Bessel beams.

Keywords: Gaussian–Bessel beams, phase object, Z-scan
PACC: 4225B, 4265

1. Introduction

Development of high power laser sources has motivated an extensive research in the study of nonlinear optical properties and optical limiting behaviour of materials. A variety of experimental methods are used for measurements of third-order nonlinear susceptibility, such as four-wave mixing,[1,2] nonlinear image techniques,[3] and Z-scan.[4] The Z-scan technique has been used as an accurate method for determining nonlinear refraction and absorption of materials. Recently, Yang *et al.*[5,6] have proposed a Z-scan method with a phase object (PO) by using Gaussian beams. By using this method, the sign of the refractive index can be easily derived from the closed aperture Z-scan curve.[5] Moreover a single-shot measurement of nonlinearity is developed with a PO.[6] Recently, the non-Gaussian beams have drawn a lot of attention for their peculiar propagation properties.[7−11] Hughes and Burzler investigated the theory of Z-scan measurement with Gaussian–Bessel (GB) beams.[12] They found that even the slightest deviation from a perfect Gaussian beam can change the sensitivity of the measurements significantly. And they demonstrate that with GB beams the Z-scan sensitivity can be enhanced significantly. In this paper, we have carried out theoretical studies of Z-scan technique by using GB beams with a PO. Using this method, we can determine both the sign and amplitude of the nonlinear coefficients with high sensitivity. Also, we compare the sensitivity of this method with GB beams and Gaussian beams Z-scan technique.

2. The Gaussian–Bessel beams Z-scan technique with a PO

In Z-scan measurements, the sample is moved along the propagation direction (z-axis) of a tightly focused beam, and the variation of far-field intensity is used to determine the nonlinear refraction of the sample. Although Z-scan has the simplicity of both experimental setup and data analysis, a high-quality Gaussian TEM_{00} beam for absolute measurements is required. Any distortions of the profile of the Gaussian beam would cause the reduction of sensitivity. In this work, we focus our attention on non-Gaussian (that is GB) beam Z-scan technique with a PO, because the GB Z-scan with a PO has high sensitivity to determine the nonlinear refractive index. The gen-

*Project supported by the National Natural Science Fundation of China (Grant No. 90922007).
†Corresponding author. E-mail: ylsong@hit.edu.cn
© 2010 Chinese Physical Society and IOP Publishing Ltd

eration and uses of diffraction-free beams have been subjects of extensive studies in the past decades. Durmin and his co-workers first demonstrated the GB beam theoretically and experimentally in 1987.[13,14] The proposed new type of diffraction-free beam posseses nearly non-diffracting behaviour: its profile is nearly unchanged within some distance. The profile of the beam has transverse distributions of the form of a Bessal function of the first kind and zero order, and it can be obtained experimentally by arranging diffraction form of a circular slit. Following Ref. [15], we obtain the electronic field of GB beam as:

$$E(r,t) = E_0 J_0(\zeta r)\exp(-r^2/\omega_0^2)\exp\left(-\frac{t^2}{2\tau^2}\right), \quad (1)$$

where $\omega_0 = 34$ μm is the radius of the focal spot (half width e^{-2} maximum irradiance) of a Gaussian beam, E_0 is the amplitude of the electric field. The profile of the beam is modified by ζ, where ζ^{-1} is the central maximum width of the Bessel beam. The profile of the beam reduces to an ordinary Gaussian beam for $\zeta = 0$. The Z-scan technique with a PO has been described in detail by Yang *et. al.*[5]

In our work, we substitute the Gaussian beam with GB beam to investigate the sensitivity of GB Z-scan technique with PO. The experimental setup for the GB Z-scan with PO method is shown in Fig. 1. Briefly, the GB laser beam first passes through lens L_1 with a focal length of 40 cm and a PO which is arranged at the focal plane of L_1. Then the GB beam is split by the beam splitter (BS) and is directed a small portion of the incident beam to the detector D_1, which monitors the fluctuation of the incident pulse energy. The rest of the pulse is tightly focused by a lens and transmits through the sample at various positions (Z) relative to the beam waist at $Z = 0$. We normalize the values of D_2, which monitors the transmitted energy, with the corresponding values obtained in linear regime (at the starting Z), which yields the normalized transmitted energy (NT). The radius of the PO is $L_p = 0.5$ mm, and phase retardation is $\phi_L = 0.5\pi$ as shown in Fig. 2. In our study, we use 19-ps laser full width at half maximum (FWHM) with the wavelength of 532 nm. A well known sample CS_2 is used to demonstrate our method. The change of refractive index can be assumed as $\Delta n = \gamma I$. The nonlinear parameter was taken to be $\gamma = 3.2 \times 10^{-14}$ cm^2/W.[16] The sample is in a 2 mm thick cell and the sample-detector distance is $d = 2f = 80$ cm.

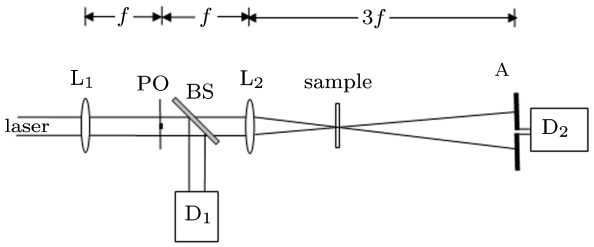


Fig. 1. The schematic diagram for GB Z-scan measurement with a PO. The L_1 and L_2 are the same convex lenses, D_1 and D_2 are detectors, A is aperture, BS stands for beam splitter.

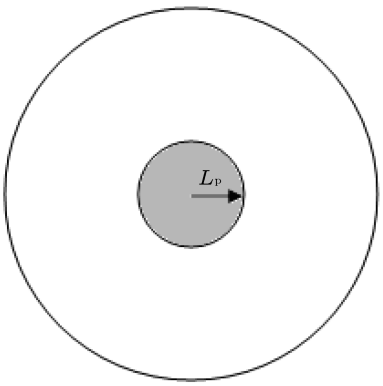


Fig. 2. The schematic diagram of the PO.

With the help of the Fresnel diffraction formula, the electric field on the front surface of the lenses L_1 can be expressed as[15]

$$E_1(r_1,t) = E_0(r_1,t)\frac{\omega_0}{\omega(f)}\exp\{\mathrm{i}[(k-\zeta^2/2k)f - \Phi(f)]\}J_0[\zeta r_1/(1+\mathrm{i}\,f/L)] \times \exp\{[-1/\omega^2(f) + \mathrm{i}\,k/2R(f)](r_1^2 + \zeta^2 f^2/k^2)\}, \quad (2)$$

where $L = k\omega_0^2/2$ is the Gaussian beam diffraction length, $R(f)=1+L^2/f^2$ is the radius curvature, $\Phi(f) = \arctan(f/L)$ is the z-dependent phase, and $\omega(f) = \omega_0[1 + (f/L)^2]^{1/2}$. The electric field on the rear surface of L_1 is

$$E_2(r_1,t) = E_1(r_1,t)\exp\left(-\frac{\mathrm{i}\,kr_1^2}{2f}\right). \quad (3)$$

Using the Fresnel diffraction formula, we derive the output electric field of the PO as

$$E_3(r_2,t) = \exp(\mathrm{i}\,\varphi_{\mathrm{L}}\mathrm{circ}(r_2/L_{\mathrm{p}})) \times\frac{\mathrm{e}^{\mathrm{i}\,kf_1}\mathrm{e}^{\mathrm{i}\,kr_2^2/2f}}{\mathrm{i}\,\lambda f}\int_0^{\infty}2\pi r_1E_2(r_1,t) \times\mathrm{e}^{\mathrm{i}\,kr_1^2/2f}J_0(r_1r_2)\mathrm{d}r_1. \quad (4)$$

Similarly, the electric field of the front surface of L_2 is derived as

$$E_4(r_3,t) = \frac{\mathrm{e}^{\mathrm{i}\,kf_2}\mathrm{e}^{\mathrm{i}\,kr_3^2/2f}}{\mathrm{i}\,\lambda f}\int_0^{\infty}2\pi r_2E_3(r_2,t) \times\mathrm{e}^{\mathrm{i}\,kr_2^2/2f}J_0(r_2r_3)\mathrm{d}r_2. \quad (5)$$

And the output electric field of the rear surface of L_2 is

$$E_5(r_3,t) = E_4(r_3,t)\exp\left(-\frac{\mathrm{i}\,kr_3^2}{2f}\right). \quad (6)$$

The incident electric field on the sample for different z position is given by

$$E_5(r_4,z,t) = \frac{\mathrm{e}^{\mathrm{i}\,kz}\mathrm{e}^{\mathrm{i}\,kr_4^2/2z}}{\mathrm{i}\,\lambda z}\int_0^{\infty}2\pi r_3E_4(r_3,t) \times\mathrm{e}^{\mathrm{i}\,kr_3^2/2z}J_0(r_3r_4)\mathrm{d}r_3. \quad (7)$$

The equations governing the irradiance and phase changes are

$$\frac{\mathrm{d}I}{\mathrm{d}z'} = -\alpha_0 I - \beta I^2, \quad (8)$$

$$\frac{\mathrm{d}\Delta\phi}{\mathrm{d}z'} = k\Delta n, \quad (9)$$

where $\Delta\phi$ is the phase changes, and z' the penetration depth. α_0 and β denote the linear absorption coefficient and two photon absorption coefficient respectively. The irradiance of the electric field is

$$I = |E_5(r_4,z,t)|^2. \quad (10)$$

The electric field on aperture plane can be given by

$$E_6(r_5,z,t) = \frac{\mathrm{e}^{\mathrm{i}\,kz}\mathrm{e}^{\mathrm{i}\,kr_5^2/2d}}{\mathrm{i}\,\lambda d}\int_0^{\infty}2\pi r_4E_5(r_4,z,t) \times\mathrm{e}^{\mathrm{i}\,kr_4^2/2d}J_0(r_4r_5)\mathrm{d}r_4. \quad (11)$$

The transmitted energy through the aperture A_2 obtained by spatially integrating $E_6(r_5,z,t)$ up to aperture radius r_a is

$$P_c = \int_{-\infty}^{+\infty}\int_0^{r_a}2\pi r_5\left|E_6(r_5,z,t)\right|^2\mathrm{d}r_5\mathrm{d}t. \quad (12)$$

Also, the aperture can be removed and the corresponding transmitted energy is

$$P_{op} = \int_{-\infty}^{+\infty}\int_0^{+\infty}2\pi r_5\left|E_6(r_5,z,t)\right|^2\mathrm{d}r_5\mathrm{d}t. \quad (13)$$

Similarly, assuming $\beta = 0$ and $\gamma = 0$, we derive linear transmitted energy $P_{\mathrm{c}0}$ and $P_{\mathrm{op}0}$. The closed and open aperture normalized transmittances are given by $NT_{\mathrm{c}} = P_{\mathrm{c}}/P_{\mathrm{c}0}$ and $NT_{\mathrm{op}} = P_{\mathrm{op}}/P_{\mathrm{op}0}$ respectively. Although the exact expression of the normalized transmittance can not be given, but numerical simulation can be taken to fit the experimental results with help of the equations mentioned above.

3. Results and discussion

Using the equations mentioned above, we theoretically simulated the experimental results of the GB Z-scan method with a PO. Using the pulse energy of 0.03 μJ, $\beta = 0$, $L_{\mathrm{p}} = 0.5$ mm, $r_{\mathrm{a}} = 2L_{\mathrm{p}}$, $\zeta = 0.11\ \mu\mathrm{m}^{-1}$ and $\gamma = \pm 3.2\times10^{-14}\ \mathrm{cm}^2/\mathrm{W}$, we derive the theoretical lines, as shown in Fig. 3(a). The single 'peak' curve indicates positive refractive index and the single 'valley' curve represents negative refractive index. It is different from the conventional Z-scan technique, which is used to judge the sign of the refractive index by the 'peak–valley' or 'valley–peak' shape of the curve. In the conventional Z-scan technique, the refractive index change causes the laser beam broadening or narrowing in the far field, and results in the transmittance change of the aperture. However, in the Z-scan experiment with a PO, the refractive index change of the beam results in the amplitude change of the beam inside the PO diffraction zone. To obtain high accuracy, appropriate radius of aperture should be adjusted. In our arrangement, the diffraction image edge of the PO is adjusted to coincide with the edge of the aperture for obtaining high sensitivity. When we set ζ=0 $\mu\mathrm{m}^{-1}$, $\phi_L = 0$, and keep other conditions unchanged, the theoretical results represented the traditional Z-scan with perfect Gaussian beam are obtained in Fig. 3(b). As can be recognized from the figures, the ΔT of the GB beam Z-scan with a PO is 60 times greater than that of the Gaussian beam even though their input profiles appear to be very similar at $Z = 0$ position, as can be seen in Fig. 4. The Z-scan technique with a GB beam offers substantial improvement over conventional Z-scan measurements by exploiting the fact that, in the far field, the centre of the GB beam suffers the largest relative irradiance change in an induced lens.

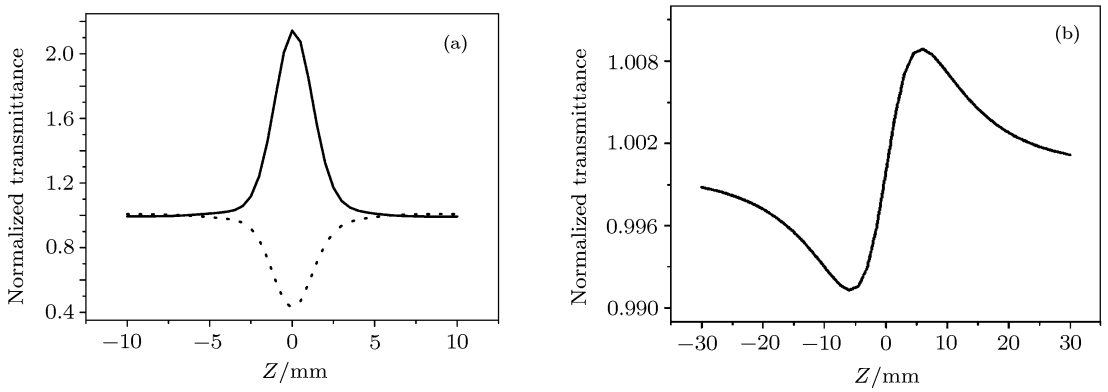


Fig. 3. (a) Normalized PO Z-scan curve f GB ($\zeta = 0.11\ \mu\text{m}^{-1}$) results with input pulse energy of 0.03 μJ for $\gamma = \pm 3.2 \times 10^{-14}$ cm^2/W. The solid line denotes the positive refraction and the dotted line represents the negative refraction. (b) Normalized Z-scan curve of Gaussian beam with input pulse energy of 0.03 μJ for $\gamma = 3.2 \times 10^{-14}$ cm^2/W.

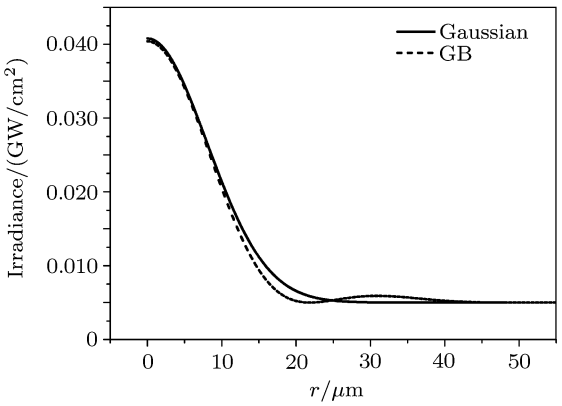


Fig. 4. Transverse irradiance distribution (at the focal plane of L_2) of a GB beam ($\zeta = 0.11\ \mu\text{m}^{-1}$) and a Gaussian beam.

The sensitivity of GB Z-scan with a PO will be enhanced by changing the parameter ζ which agrees well with the results shown in Ref. [12]. Moreover we investigate the sensitivity of GB Z-scan with a PO by changing L_p and r_a. When we fix the sample at the $Z = 0$ position with the optimal sensitivity condition $r_\text{a} = 2L_\text{p}$, the normalized transmittance with respect to L_p is obtained in Fig. 5. As can be recognized from this figure, $L_\text{p} = 0.25$ mm is optimal for the best sensitivity.

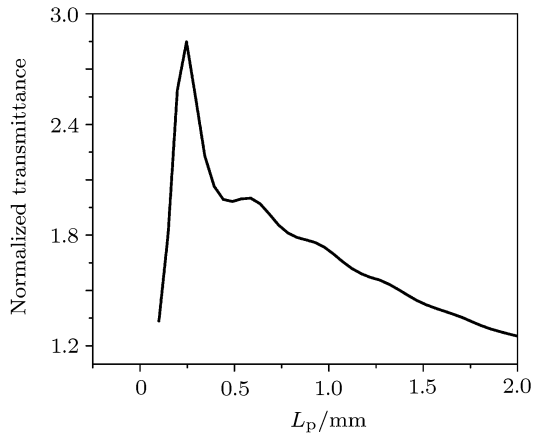


Fig. 5. Normalized transmittance versus L_p at the $Z = 0$ position.

With the same input pulse energy of 0.03 μJ and $L_\text{p} = 0.25$ mm, we theoretically simulate the GB Z-scan results without a PO, and compare it to this PO Z-scan method. As can be seen from Fig. 6, the ΔT of GB Z-scan results with a PO is 2 times greater than that of GB Z-scan results indicating that this method has higher sensitivity in measuring the nonlinear refractive index. Moreover, with the increase of the input pulse energy the sensitivity will enhance more, and the results are shown in Fig. 7. The adding of a PO in the GB Z-scan strongly changes the interference of the beam in the far field at the PO zone. The laser beam induced refraction change is converted into amplitude change in the PO zone. It is just like the principle of phase contrast. To highlight this scenario, we depict in Fig. 8 the resulting far-field GB and that with a PO transverse profile at the detector plane. As can be recognized from the figure, the fluence at the centre of the far-field of the GB with a PO is higher than that of GB. The centre of the beam represents most information of the refraction changes induced by the sample–laser interaction, because of the high intensity at the centre of the beam. The GB Z-scan with a PO has higher energy fluence at the centre of the far field, which indicates that the GB Z-scan method with a PO has higher sensitivity than that of GB Z-scan. We conclude that the high sensitivity of the GB Z-scan is achieved by changing the post-sample of the

electric field. However, it does not need an obstruction disk that blocks most of the light. In our study, the adding a PO modulates the post-sample electric field, and subsequently changes the sensitivity.

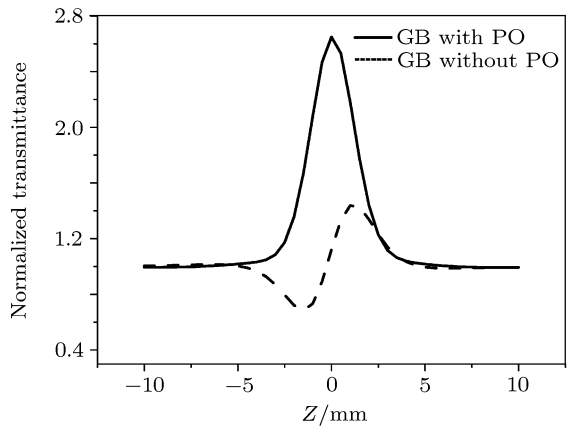


Fig. 6. Normalized GB ($\zeta = 0.11\ \mu\text{m}^{-1}$) Z-scan with a PO (solid line) and GB Z-scan (dashed line).

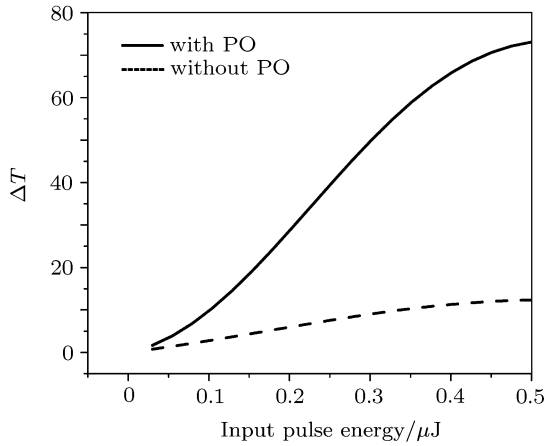


Fig. 7. Normalized ΔT versus the input pulse energy for the GB Z-scan with a PO and GB Z-scan.

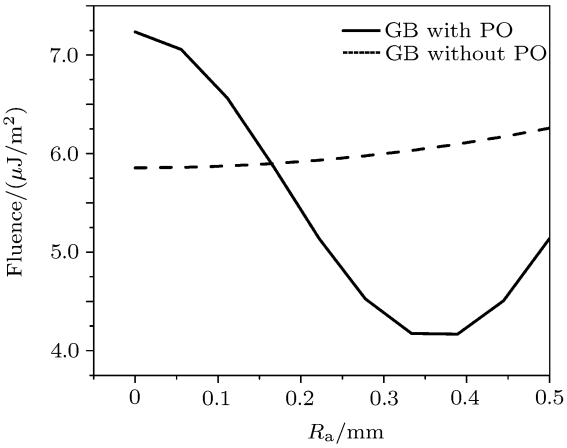


Fig. 8. Transverse far-field energy fluence distribution (at the detector plane) of GB beam and GB beam with a PO.

4. Conclusion

We theoretically investigated a GB Z-scan method with a PO to investigate the third order nonlinearities. The proposed method is advantageous for the high sensitivity in measuring the nonlinear refractive index. It imposes a lower stress in the cases of fragile materials, since a small laser pulse will gain high sensitivity. Meanwhile, we can simply distinguish the sign of the refractive index of nonlinear materials from the single 'peak' or 'valley' shape of Z-scan curves.

References

[1] Sutherland R L, McLean D G and Kirkpatrick S 1996 *Handbook of Nonlinear Optics* (New York: Marcel Dekker)

[2] Friberg S R and Smith P W 1987 *IEEE J. Quantum Electron.* **23** 2089

[3] Boudebs G, Chis M and Bourdin J P 1996 *J. Opt. Soc. Am.* B **13** 1450

[4] Sheik-Bahae M, Said A A, Wei T H, Hagan D J and Van Stryland E W 1990 *IEEE J. Quantum Electron.* **26** 760

[5] Yang J Y and Song Y L 2009 *Opt. Lett.* **34** 157

[6] Yang J Y, Song Y L, Jin X, Shui M and Li C W 2010 *Chin. Phys.* B **19** 024201

[7] Hakola A, Buchter S C, Kajava T, Elfström H, Simonen J, Pääkkönen P and Turunen J 2004 *Opt. Commun.* **238** 335

[8] Cai Y J, Chen C Y and Wang F 2007 *Opt. Commun.* **278** 34

[9] Chen B S and Pu J X 2009 *Chin. Phys.* B **18** 1033

[10] Zhou G Q, Chen L and Chu X X 2007 *Chin. Phys.* **16** 2709

[11] Lu Z D 2007 *Chin. Phys.* **16** 1320

[12] Hughes S and Burzler J M 1997 *Phys. Rev.* A **56** 1103

[13] Durnin J 1987 *J. Opt. Soc. Am.* A **4** 651

[14] Durnin J, Miceli J J and Eberly J H 1987 *Phys. Rev. Lett.* **15** 1499

[15] Gori F, Guattari C and Padovani C 1987 *Opt. Commun.* **6** 491

[16] Willianms W E, Soileau M J and Van Stryland E W 1984 *Opt. Commun.* **50** 256